

# Turbine Speed Control for an Ocean Wave Energy Conversion System

Paula B. Garcia-Rosa, José Paulo V. S. Cunha and Fernando Lizarralde

**Abstract**—In this work, a hydraulic turbine speed governor is proposed in view of its application in an isolated electric generation system based on an ocean wave energy converter (WEC). The proposed strategy is based on cascade closed-loop control combined with feedforward of load disturbances. The main characteristics of a WEC are presented and a dynamic model of the generating unit is developed. Experimental results illustrate the performance of the proposed control scheme.

**Index Terms**—Ocean wave energy, Cascade control, Feedforward control, Pelton turbine, Speed governor.

## I. INTRODUCTION

The use of renewable sources to produce electricity represents an alternative to meet the growing energy demand and reduce global  $CO_2$  emissions. In this context, the ocean wave energy has been considered an interesting solution to islands or countries with large coastal areas [1].

Nowadays, the wave energy converters (WECs) are in different stages of development. They are usually based on the following principles of energy conversion [1]: (i) *Oscillating Water Column (OWC)*: the wave action makes the water level in an air chamber oscillate. Then, the air in the chamber is compressed and expanded generating an air flow through a Wells turbine coupled to an electrical generator; (ii) *Oscillating Bodies*: the buoy movement generated by the wave actions compress water (or oil) through hydraulic cylinders. The compressed fluid flows through turbines or motors coupled to generators. Some examples of these technologies are the OWC Plant on the Pico Island, the LIMPET Converter, the Energetech OWC, the Pelamis Wave Energy Converter and the Archimedes Wave Swing [1].

This paper considers an oscillating body WEC proposed by the Submarine Technology Laboratory at COPPE/Federal University of Rio de Janeiro (Brazil), which applies a hyperbaric chamber and a conventional Pelton turbine coupled to an electric generator [2].

The electric generator can be connected to the power grid or, to an isolated system. In this framework, the system should be maintained at the normal operation state, even in the presence of variations in the load demand. The quality of the electricity supplied must meet requirements with respect to limits of variations in frequency and voltage, as well as the level of reliability [3]. For these purposes, voltage and frequency (speed) controllers can be applied in synchronous

generators or other controllable equipments located in the electric power grid, when the energy source is highly variable, as in wind or wave energy. Note that in the considered WEC, the hyperbaric chamber act as an energy storage system, which smooths incoming power variations due to changes on the sea state. Then, the traditional techniques generally used in hydropower plants can be considered to obtain an acceptable power quality.

Frequency and voltage control can be simplified by the natural decoupling between pairs of the following variables: active power/frequency and reactive power/voltage. Therefore, within the normal range of operation, the flow of active and reactive power can be considered independent of each other and influenced by different control actions [3]. In this work, the problem of frequency (speed) control of an isolated wave energy system is addressed. Then, to regulate the speed, the generated power is controlled by changing the water flow by means of a distributor, which injects water into the turbine blades. Usually, the actuator of a speed governor is the distributor.

Isolated and small systems are difficult to control [4], since the system inertia is small and there is only one or few generators connected to the load to restore the system frequency. Therefore, fast rates of speed changing can occur when there is an abrupt load disturbance. Thus, to keep the operation of these systems within acceptable limits of frequency deviation ( $\pm 2\%$ ) [5], the controller must be able to reduce speed deviation during transients.

In reference [6], an electronic load governor is proposed for a mini-hydroelectric power plant. However, this solution requires additional power electronics equipment.

On the other hand, high-gain control can be used to maintain the turbine speed insensitive to load disturbances. However, the use of high gains may destabilize the system [7]. In references [7], [8], overspeed controllers with proportional and integral (PI) actions combined with feedforward control are applied to a small hydroelectric power plant. The use of feedforward allows the reduction of the PI gains such that the gain margin is increased in order to avoid oscillations and stability problems.

In this paper, a cascade closed-loop controller plus feedforward of load disturbances is proposed for the turbine speed control of an isolated WEC. The performance of the proposed control scheme is illustrated by experimental results obtained with a small prototype.

This work was partially supported by CNPq, CAPES and FAPERJ, Brazil.

P. B. Garcia-Rosa and F. Lizarralde are with the Dept. of Electrical Eng., COPPE, Federal University of Rio de Janeiro, Brazil, paula@coep.ufrj.br, fernando@coep.ufrj.br.

J. P. V. S. Cunha is with Department of Electronics and Telecommunication Engineering, State University of Rio de Janeiro, Brazil, jpaulo@ieee.org.

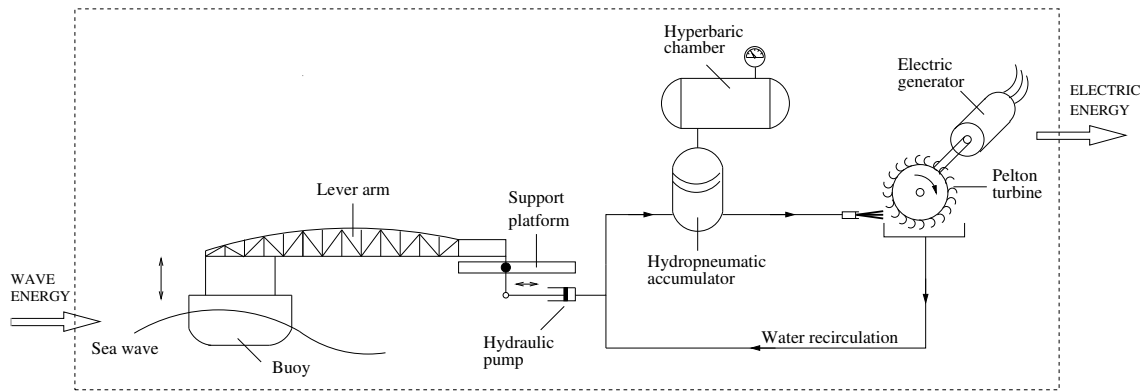


Fig. 1. Scheme of the wave energy converter system.

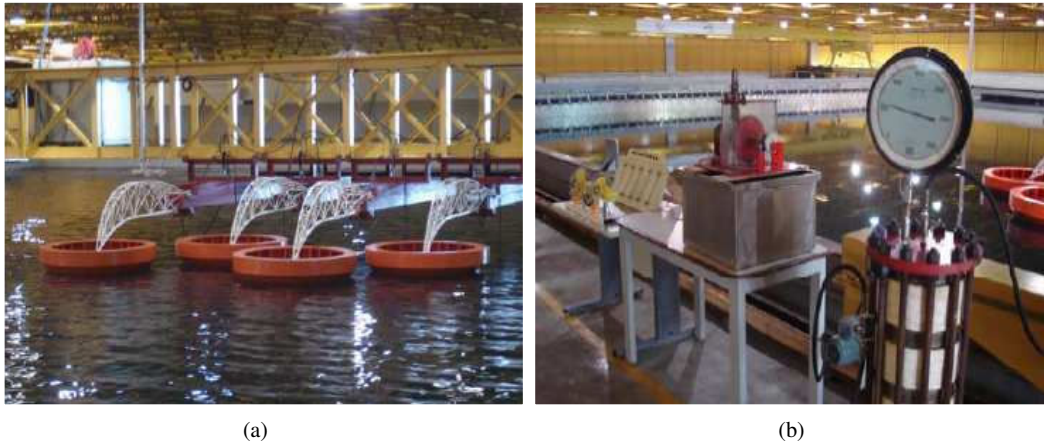


Fig. 2. Wave energy converter system at LabOceano: (a) small-scale pumping modules; (b) small turbine and hydropneumatic accumulator.

## II. WAVE ENERGY HYPERBARIC CONVERTER FOR ELECTRICITY PRODUCTION

The wave energy hyperbaric converter shown in Fig. 1 consists of pumping modules connected to a generating unit, which is composed of a hyperbaric chamber, a hydropneumatic accumulator, a hydraulic turbine and an electrical generator.

Each pumping module has a buoy linked to a hydraulic pump through a lever arm. The vertical motion of the buoy, due to the wave action, induces the pump to displace water obtained from a closed circuit to the hydropneumatic accumulator. The output flow of water from this accumulator is released in the form of a jet, which moves a Pelton turbine coupled to the electrical generator [2]. The hydropneumatic accumulator stores water at high pressure. It provides an approximately constant hydraulic pressure, even with variations in the waves and in the stored water level, since it is connected to a large hyperbaric chamber filled with nitrogen.

Figure 2 presents a small-scale prototype of the WEC system tested in the ocean basin (LabOceano) at the Federal University of Rio de Janeiro (Brazil). Figure 2.a presents the small-scale (1:10) pumping modules. In these tests, the hydropneumatic accumulator (Fig. 2.b) has been previously pressurized with nitrogen gas.

## III. DYNAMIC MODEL OF THE GENERATING UNIT

It is assumed that the hyperbaric chamber smooths the variations in the power absorbed by the buoys, such that the pressure in the hydropneumatic accumulator is constant. Therefore, the generating unit of this system can be modeled similarly to generating units of hydroelectric power plants, since the chamber maintains the pressure high and the energy conversion processes of these units are similar.

For the purposes of speed governor analysis and design, the plant model should consider the dynamics of the turbine, which includes the water dynamics in the conduit, and the dynamics of the rotor (Fig. 3) [9]. This section describes

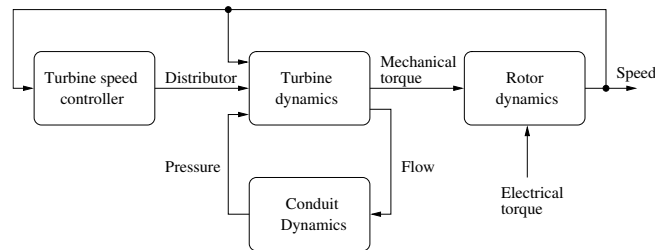


Fig. 3. Basic structure of a generating unit.

the distributor dynamic model, which is a needle for Pelton

turbines, a linearized hydraulic turbine model including the conduit and rotor dynamics.

#### A. Needle Dynamics

The needle is mechanically coupled to a DC servomotor. Since the motor shaft rotation results in a linear displacement of the needle, a model of this electromechanical actuator is given by the transfer function [10]

$$G_1(s) = \frac{X_n(s)}{U(s)} = \frac{K_n}{s(T_n s + 1)}, \quad (1)$$

where

$$K_n = \frac{k_m k_r k_o}{R_a b + k_m^2}, \quad T_n = \frac{R_a J}{R_a b + k_m^2}, \quad k_o = \frac{U_o}{X_{no}},$$

$X_n$  is the normalized needle position (per unit — pu),  $X_{no}$  is the base needle position (m),  $U$  is the normalized servomotor voltage (pu),  $U_o$  is the base servomotor voltage (V) and  $k_r$  is ratio between the linear displacement of the needle and the corresponding motor shaft rotation (m/rad). The parameters of servomotor are the torque coefficient  $k_m$  (Nm/A), the armature resistance  $R_a$  ( $\Omega$ ), the equivalent moment of inertia  $J$  ( $\text{kg m}^2$ ), and the viscous friction coefficient  $b$  (Nms/rad).

#### B. Hydraulic Turbine Dynamics

A linearized model of a hydraulic turbine can be obtained considering the following assumptions [3]:

- (A1) The water is incompressible and the conduit is inelastic;
- (A2) The pressure loss in the distributor and conduit are negligible;
- (A3) The water speed in the conduit is directly proportional to the distributor opening and the square root of the water column height (which, in this case, is proportional to the accumulator pressure);
- (A4) The mechanical power of the turbine is proportional to the product of pressure and water flow through the turbine.

Then, considering assumptions (A1)-(A4), the linearized model of the hydraulic turbine, for small signals about an operating point, is given by the transfer function

$$G_2(s) = \frac{\Delta P_m(s)}{\Delta X_n(s)} = \frac{1 - T_w s}{1 + \frac{1}{2} T_w s}, \quad T_w = \frac{L Q_0}{g A_L H_0}, \quad (2)$$

where  $\Delta P_m$  is the incremental change of the turbine mechanical power (pu),  $\Delta X_n$  is the incremental change of the needle position (pu),  $T_w$  is the water inertia time constant (s),  $L$  is the length of the conduit (m),  $A_L$  is the cross section area of the conduit ( $\text{m}^2$ ),  $g$  is the gravity acceleration ( $\text{m/s}^2$ ),  $Q_0$  is the rated value of water flow ( $\text{m}^3/\text{s}$ ) and  $H_0$  is the equivalent water column height (m).

The transfer function (2) gives the relationship between the turbine mechanical power and the distributor position for ideal lossless turbines. In the considered WEC, the conduit can be designed to keep  $T_w$  small such that the turbine power response to distributor commands is fast enough for improved control performance. For this purpose, the turbine

must be installed near the hydropneumatic accumulator. A short conduit (small  $L$ ) with large cross section area ( $A_L$ ) is desirable to reduce non-minimum phase effects [4].

In this WEC, the conduit length is  $L = 3 \text{ m}$ . Then, using the expression  $T_w = L Q_0 / g A_L H_0$ , one estimates that  $T_w$  is 0.07 s, which is relatively small compared to hydroelectric plants, where the constant  $T_w$  typically varies from 0.5 s to 4 s, resulting in significant non-minimum phase effects.

For example, in the small hydroelectric system described in [7], [8], the needle movements must be slow to reduce pressure oscillations due to the long conduit. Therefore, the control is achieved through deflectors that can divert the water jet and reduce the mechanical power quickly [7]. Of course, deflectors cause undesirable energy losses and their use can be avoided in this WEC system since  $T_w$  is small.

#### C. Rotor Dynamics

The rotor dynamics includes the electrical generator and the electric load. Considering an isolated generating unit supplying a local load, the rotor motion satisfies the following differential equation

$$\Delta \dot{\omega} = \frac{1}{T_m} (\Delta P_m - \Delta P_e), \quad T_m = \frac{J_m \omega_0^2}{P_0}, \quad (3)$$

where  $\Delta P_m$  is the incremental change of the mechanical power on the turbine shaft (pu),  $\Delta P_e$  is the incremental change of the generated electric power (pu),  $P_0$  is the rated power of the generator (W),  $\Delta \omega$  is the incremental change of the rotor speed (pu),  $\omega_0$  is the base speed (rad/s),  $J_m$  is the combined moment of inertia of the generator and turbine ( $\text{kg m}^2$ ) and  $T_m$  is the mechanical inertia time constant (s).

The electrical power of the generator can be modeled by a constant power term and a frequency dependent term [3],

$$\Delta P_e = \Delta P_L + D_p \Delta \omega, \quad (4)$$

where  $\Delta P_L$  is the incremental change in the electric load (pu) and  $D_p$  is the load-damping constant (pu).

Then, from (3) and (4) the linearized model of the rotor is given by the transfer function

$$G_3(s) = \frac{\Delta \omega(s)}{\Delta P_m(s) - \Delta P_L(s)} = \frac{1}{T_m s + D_p}. \quad (5)$$

In the absence of a speed governor, the system response to load disturbances is defined by the rotor inertia ( $J_m$ ) and the damping constant ( $D_p$ ).

## IV. SPEED GOVERNOR

The main objective of a speed governor is to regulate the turbine speed at the rated value,  $\omega_{ref}$ , so that the generated power equals the load power. In the presence of load disturbances, the governor should reduce speed changes and, consequently, avoid the frequency to reach unacceptable values. Hence, the following criteria is established for the controller design: the steady state error of the turbine speed (in case it occurs) and the speed deviation during transients should be kept within the admissible tolerance ( $\pm 2\%$ ) [5].

In this context, a cascade controller combined with feed-forward of the measured load power is proposed in order to

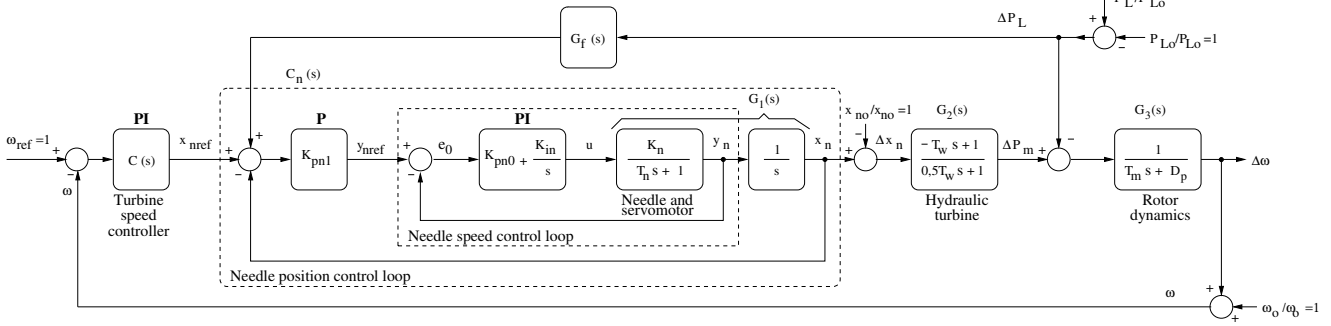


Fig. 4. Block diagram of the proposed turbine speed governor. Water pressure disturbance signals are not shown to avoid clutter.

regulate the speed of a Pelton turbine. Figure 4 shows the block diagram of the proposed controller.

#### A. Cascade Controller

A P-PI cascade controller [10] is adopted for the needle position control (inner loop) and a PI controller is adopted for turbine speed regulation (outer loop), see Fig. 4.

The tuning of the needle control loop has to be performed before the turbine speed control tuning. The adjustment of gains  $K_{pn0}$ ,  $K_{in}$  and  $K_{pn1}$  is based on pole placement. First, the internal loop is tuned (needle speed control) and then, the external loop (position control).

Gains  $K_{pn0}$  and  $K_{in}$  are determined such that the two closed-loop poles are located at  $p_2 = cp_1$ , where  $p_1$  is the desired P-PI dominant pole and  $c > 1$  is a design constant. From the internal loop characteristic equation

$$s^2 + \left( \frac{K_n K_{pn0} + 1}{T_n} \right) s + \frac{K_n K_{in}}{T_n} = 0, \quad (6)$$

the gains can be calculated by

$$K_{pn0} = -\frac{2T_n cp_1 + 1}{K_n}, \quad K_{in} = \frac{T_n}{K_n} c^2 p_1^2. \quad (7)$$

The  $K_{pn1}$  gain is chosen such that the dominant pole  $p_1$  of the needle position control loop has faster dynamics than the turbine control loop. Thus, the gain  $K_{pn1}$  is given by

$$K_{pn1} = \frac{p_1^2(2c - c^2 - 1)}{c^2 - 2cp_1 - T_n^{-1}}. \quad (8)$$

The turbine PI speed regulator is given by

$$C(s) = K_p + \frac{K_i}{s}, \quad (9)$$

where the gains  $K_p = 0.0022$  and  $K_i = 0.001$  are adjusted according to the performance criteria established in Sec. IV. The resulting gain margin is 25 dB and the phase margin is 55°.

In the presence of large load disturbances, the needle speed reference signal ( $y_{nref}$ ) has to be saturated in order to limit the maximum speed of the needle displacement ( $y_{nmax}$ ), since in this case, the feedforward control action may demand fast displacements of the needle. Thus, an antireset windup strategy can be adopted to avoid the excessive growth of the integral action, when voltage saturation occurs in the servomotor terminals.

#### B. Feedforward Control

In order to attenuate disturbance effects and reduce turbine speed changes, a feedforward action is added to the control structure as shown in Fig. 4. This strategy provides an anticipatory corrective action, which partially compensates the effects of disturbances before the closed-loop controller actuates significantly. The load electrical power ( $P_L$ ) is estimated from measure of voltage and current.

According to [11], a feedforward compensator should ideally be given by the inverse of part of the nominal plant model, i.e.,

$$G_f(s) = [C_n(s) G_2(s)]^{-1}, \quad (10)$$

where  $C_n(s)$  is the transfer function of the needle position control loop (see Fig. 4). As the inverse of  $C_n(s)G_2(s)$  is nonrealizable, since it is unstable (due to the non-minimum phase of  $G_2(s)$ ) and noncausal,  $G_f(s)$  is approximated by the static gain

$$G_f(s) \approx K_f = [C_n(0) G_2(0)]^{-1} = 1. \quad (11)$$

This is a good approximation provided that the needle control loop is fast enough and the time constant  $T_w$  in (2) is small.

#### V. SIMULATIONS

In this section, simulation results are presented in order to evaluate the performance of the proposed control scheme in terms of settling time, steady state error and speed deviations caused by load disturbances.

The linear plant parameters were experimentally estimated from the voltage step response of the electromechanical actuator (needle speed/motor voltage) and from the needle position step response of the turbine (turbine speed/needle position), considering small incremental signals about an operating point. The parameters obtained are  $K_n = 0.0226$ ,  $T_n = 0.096$  s,  $T_m = 0.005$  s and  $D_p = 0.0014$ . The designed parameters of the needle controller are  $K_{pn0} = 108$ ,  $K_{in} = 1350$  and  $K_{pn1} = 1.7$ .

Figure 5 shows the response of the closed-loop system for step changes of 10% and 25% on the nominal load with ( $K_f = 1$ ) and without ( $K_f = 0$ ) feedforward.

It can be observed that without feedforward ( $K_f = 0$ ) the speed error exceeds 2% for  $\Delta P_L = 25\%$ . Thus, it is not

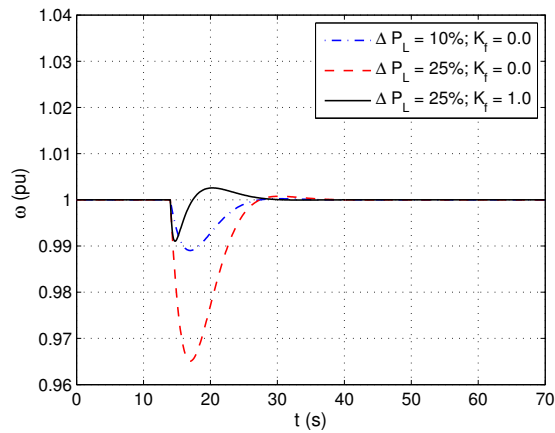


Fig. 5. Simulated rotor speed ( $\omega$ ) response to load disturbances.

possible to maintain the speed within acceptable limits for large load disturbances using only the cascade closed-loop controller. On the other hand, when the feedforward control action ( $K_f = 1$ ) is combined with the cascade controller, the speed deviation can be kept within  $\pm 1\%$ , exhibiting an overshoot of 0.4% for a load disturbance of 25%.

## VI. EXPERIMENTAL SETUP

The experimental setup in Fig. 6 is used for evaluation of the proposed control scheme. The generating system consists of a chamber, an electromechanical actuator, a Pelton turbine and an electric generator. The electric load is a set of parallel connected rheostats. As in previous experiments [2], the chamber has two compartments in which the water is isolated from the nitrogen gas, previously pressurized to form a hydropneumatic accumulator.

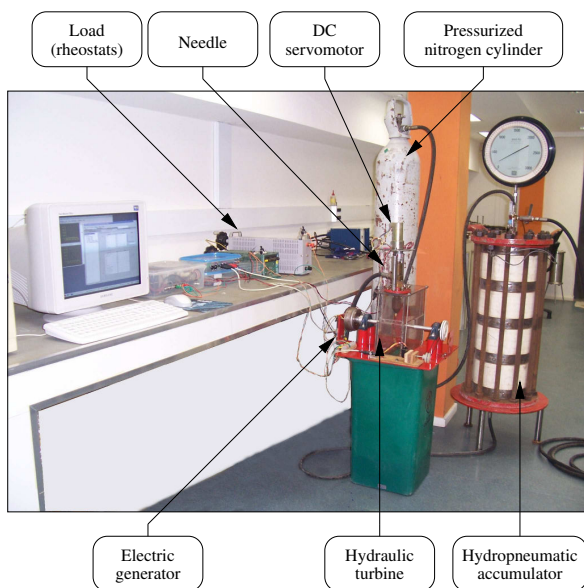


Fig. 6. Experimental setup.

The electromechanical actuator is composed of a DC servomotor (GM9234S031, Pittman Co.), a PWM driver ( $1.3\text{ A} \times 12\text{ V}$ ) and a needle. The needle position is measured by an incremental encoder coupled to the motor shaft. The turbine speed is also estimated by an incremental shaft encoder (HEDM 5500, HP Inc.).

The control algorithm is coded in C language and implemented on a DSP (Digital Signal Processor) board with 0.01 s sampling interval. This board has a TMS320C31 processor and integrated encoder inputs as well as a D/A converter that drives the motor which moves the needle. This is installed in a Linux box and the data transfer is handled by a Java Interface.

## VII. EXPERIMENTAL RESULTS

The experimental results are shown in Figs. 7 and 8. It can be observed that the turbine speed takes approximately 25 s to resume the nominal value after the system is submitted to a load change of 25%.

It can be observed in Fig. 7.a that, without the feedforward control action, the speed deviation reached approximately 5%. On the other hand, when the feedforward action is included, the deviation is less than 2% (Fig. 8.a). As expected, the feedforward action reduces the effects of load disturbances. The needle displacement is faster when this action is used and the control signal amplitude is larger, according to the comparison of Figs. 8.b–d with 7.b–d.

A steady-state error of 0.5% can be seen in Figs. 7.a and 8.a either with or without feedforward control action. The continuous needle drift observed in Figs. 7.c and 8.c compensates for the decrease of the nitrogen pressure which occurred during the experiments. This pressure variation can be considered as a ramp disturbance and causes the steady-state error observed in the turbine speed. It is expected that this disturbance will not occur in the full-scale WEC, where a large hyperbaric chamber and a hydropneumatic accumulator will maintain the pressure practically constant.

The performance of the simulated feedforward scheme in Fig. 5 is better than the experimental performance in Fig. 8.a, since the simulated feedforward provides a better estimate of the load disturbance than can be achieved in practice. Furthermore, the water pressure in the hydropneumatic accumulator is considered constant in the simulated model.

## VIII. CONCLUSIONS

In this work, an isolated ocean wave energy converter (WEC) for electricity generation is considered. A control strategy based on a combination of a cascade feedback controller with a feedforward controller has been applied for speed regulation of a hydraulic turbine.

A dynamic model of the generation unit of a WEC is developed considering approaches used in hydroelectric plants. The feedforward of the load power is applied in order to attenuate the effects of electrical load disturbances and to improve the regulation of the turbine speed. The implementation of this scheme is simple due to the small length of the conduit which supplies water to the turbine, unlike

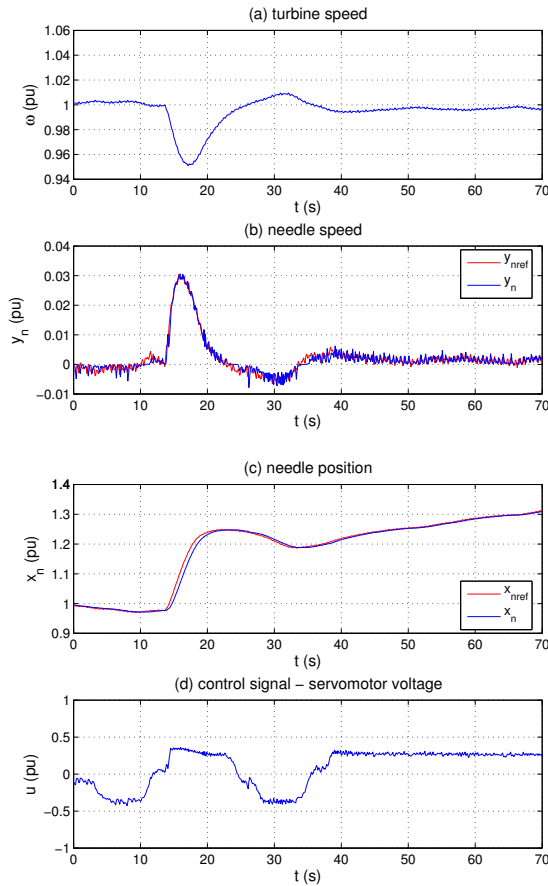


Fig. 7. Experimental results: cascade control ( $K_f = 0$ ).

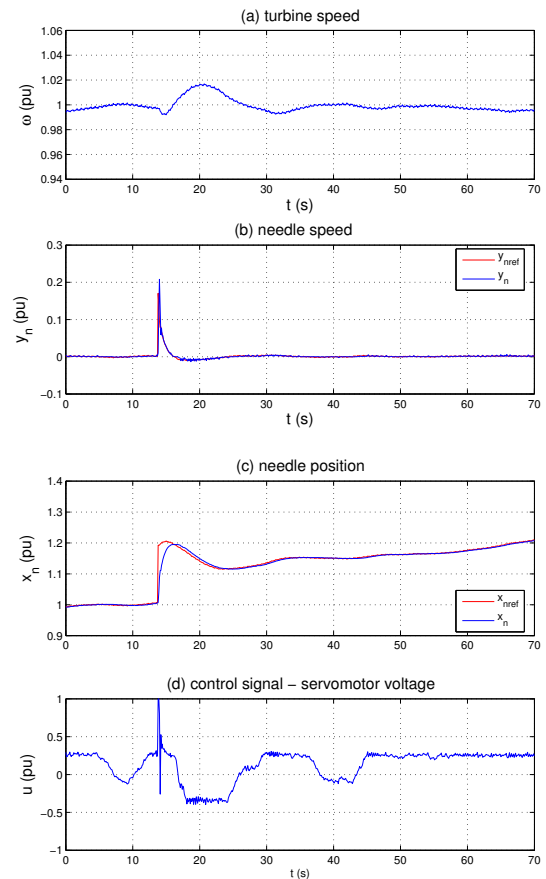


Fig. 8. Experimental results: cascade control with feedforward ( $K_f = 1$ ).

hydroelectric plants where longer conduits cause significant non-minimum phase effects which require more elaborated feedforward schemes [12] and deflectors [7], [8].

The results obtained in simulations and experiments illustrate the good performance of the proposed control scheme. It was shown that the cascade control action alone may not limit the speed deviation to acceptable levels for large load changes. Thus, a combined action with feedforward control is essential to improve the performance of the speed governor.

In future works, the dynamic effects of the hydropneumatic accumulator will be evaluated, since large variations in ocean waves are expected and may disturb the water pressure and the performance of the proposed control scheme.

## IX. ACKNOWLEDGMENTS

The authors gratefully acknowledge the support from the Submarine Technology Laboratory at COPPE/UFRJ on the experimental tests and other contributions to this work.

## REFERENCES

[1] A. Clément, P. McCullen, A. Falcão, A. Fiorentino, F. Gardner, K. Hammarlund, G. Lemonis, T. Lewis, K. Nielsen, S. Petrocini, M. T. Pontes, P. Schild, B. O. Sjöström, H. C. Sorensen, and T. Thorpe, "Wave energy in Europe: current status and perspectives," *Renewable and Sustainable Energy Reviews*, vol. 6, no. 5, pp. 405–431, October 2002.

[2] S. F. Estefen, P. R. Costa, E. Ricarte, and M. M. Pinheiro, "Wave energy hyperbaric device for electricity production," in *International Conference on Offshore Mechanics and Arctic Engineering*, vol. OMAE-2007, San Diego (CA), June 2007.

[3] P. Kundur, *Power System Control and Stability*. EPRI-Power System Engineering Series McGraw-Hill Inc., 1994.

[4] IEEE Standards, *Guide for the Application of Turbine Governing Systems for Hydroelectric Generating Units*. Power Generation Committee of the IEEE Power Engineering Society, 2004.

[5] IEC 60034-1, *Rotating electrical machines Part 1: Rating and performance*, 2004.

[6] F. Chen and K. Natarajan, "Stand alone power system frequency control," in *Proc. of the Canadian Conference on Electrical and Computer Engineering*, Ottawa, May 2006, pp. 2262–2265.

[7] R. M. Johnson, J. H. Chow, and B. Hickey, "Pelton turbine deflector control designs for Bradley Lake hydro units," in *Proc. of the American Control Conference*, vol. 6, May 2002, pp. 4855–4860.

[8] R. M. Johnson, J. H. Chow, and M. V. Dillon, "Pelton turbine deflector overspeed control for a small power system," *IEEE Trans. on Power Systems*, vol. 19, no. 2, pp. 1032–1037, May 2004.

[9] E. D. Jaeger, N. Janssens, B. Malfiet, and F. V. D. Meulebroeke, "Hydro turbine model for system dynamic studies," *IEEE Trans. on Power Systems*, vol. 9, no. 4, pp. 1709–1715, November 1994.

[10] R. Kelly and J. Moreno, "Learning PID structures in an introductory course of automatic control," *IEEE Trans. on Education*, vol. 44, no. 4, pp. 373–376, 2001.

[11] K. J. Åström and T. Häggglund, *Advanced PID Control*. ISA - The Instrumentation, Systems, and Automation Society, 2006.

[12] D. Jones and S. Mansoor, "Predictive feedforward control for a hydroelectric plant," *IEEE Trans. on Control Sys. Tech.*, vol. 12, no. 6, pp. 956–965, November 2004.